Geologie en Mijnbouw 65: 133–143 (1986)

Thermal modelling of arc-trench regions

Jilles van den Beukel & Rinus Wortel
Dept. of Theoretical Geophysics, Institute of Earth Sciences, University of Utrecht, P.O. Box 80.021, 3508 TA Utrecht, The Netherlands

Received 11 February 1986; accepted in revised form 25 May 1986

Abstract

The temperature structure of the shallow part of a subduction zone, i.e. the region between the trench and the volcanic arc, has been calculated with finite difference methods. Published heat flow measurements are used as a constraint for the thermal models. Heat flow in the arc-trench region is low ($<40\,mW\,m^{-2}$) for subduction zones which have been active for more than about 60 Ma. In the central part of the arc-trench region of these subduction zones average heat flow values range from 30 to $36\,mW\,m^{-2}$. From the thermal modelling it follows that such a heat flow level requires shear stresses of 20–60 MPa near the upper surface of the descending slab at depths between 25 and 75 km.

In addition, it is shown that the pressure-temperature relations, inferred from mineral assemblages in high-pressure metamorphic belts, can only be reached if significant heat production by friction takes place, with shear stresses similar to those inferred from heat flow data. Subduction related volcanism is caused by high temperatures in the asthenospheric wedge above the slab. It is likely that the volcanic line marks the boundary of the asthenospheric wedge.

Introduction

Several thermal models have been published of the temperature structure of a subduction zone (e.g. Minear & Toksöz 1970; Turcotte & Schubert 1973; Andrews & Sleep 1974; Anderson et al. 1978; 1980; Bird 1978; Hsui & Toksöz 1979; Sydora et al. 1980; Furlong et al. 1982; Honda & Uyeda 1983; Honda 1985). Especially for the shallow part of a subduction zone, the arc-trench region (see Fig. 1), the temperature distributions in these models exhibit large differences, mainly caused by differences in heat production by friction at the upper surface of the descending slab. Shear stresses vary from 0 MPa (Honda & Uyeda 1983) or 20 MPa (Bird 1978) up to values above 100 MPa (e.g. Turcotte & Schubert 1973; Anderson et al. 1978, 1980; Sydora et al. 1980). Generally these assumed shear stresses are rather arbitrary; only Bird (1978) bases his estimate on a force balance for two subduction zones, where back-arc spreading occurs.

The shear stresses can not be derived from the rheological properties of the material near the slip zone. Pore-fluid pressures have a large influence on rock strength in the brittle regime. Different flow laws may be chosen to model plastic deformation at higher temperatures (Yuen et al. 1978). It is not clear, to what extent subducted sediments contribute to the weakness of the material near the slip zone. In this article a different approach is chosen: temperatures (and thus shear stresses) are constrained by heat flow data. Although Anderson et

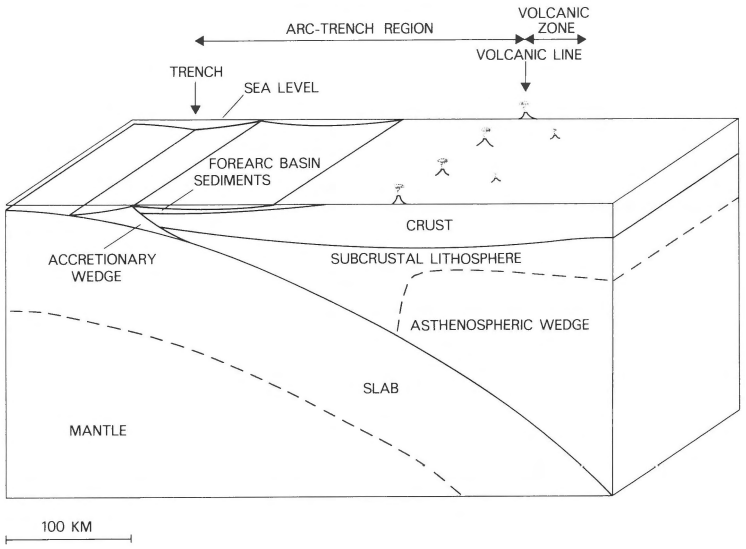

Fig. 1. The shallow part of a subduction zone. Dashed lines indicate the base of the lithosphere of the overriding plate and of the subducting plate. The vertical scale is equal to the horizontal scale.

al. (1976) already noted that the low heat flow in the region between the trench and the volcanic zone could be an important constraint for thermal models, none of the published models makes a detailed comparison between model results and observed heat flow. In view of the increased number of heat flow measurements available for subduction zones, such a comparison seems possible now.

In the model presented here, temperatures are calculated for the region between the trench and the volcanic line (arc-trench region in Fig. 1). The volcanic line is the boundary, in the direction of the trench, of the volcanic zone. The arc-trench region differs from a subduction zone as a whole, because the dip of the slab is much smaller here. Temperatures in the arc-trench region are particularly important for the evolution of continental crust near an active plate margin. High-pressure metamorphic belts are formed in the region near the trench (Miyashiro 1973; Ernst 1977). A substantial part of the continental crust may originate from subduction related volcanism (e.g. Windley 1984). Both the pressure-temperature relations for metamorphism and the place where melting (which causes volcanism) occurs are determined by the thermal structure of the arc-trench region.

Description of the model

The geometry of the model is given in Figure 2. The dip of the slab is 20° and the depth of the slab below the volcanic line is 105 km. These values are chosen in such a way that the position of a slab in the arc-trench region, as inferred from seismicity (Isacks & Barazangi 1977), is approximated as well as possible. The crustal thickness of the overriding lithosphere is 30 km; that of the descending oceanic lithosphere is 8 km.

The time dependent two-dimensional temperature distribution T(x, z, t) (where z is the depth, x the horizontal distance from the trench; T in °C) is calculated from:

$$\frac{\partial T}{\partial t} + \bar{v} \cdot \nabla T = \frac{1}{\varrho c_p} (\nabla \cdot (k \nabla T) + A) + (\frac{\partial T}{\partial t})_{ad} \quad (1)$$

For crustal material the density $\varrho = 2.7 \times 10^3$ kg m^{-3} and the thermal conductivity $k = 2.5$ W m^{-1} $°C^{-1}$. For subcrustal lithosphere and mantle the density is 3.3 kg m^{-3} and a temperature dependent thermal conductivity for olivine is used, from Schatz & Simmons (1972). The specific heat c_p is

constant throughout the model and equal to 1.05×10^3 J kg^{-1} $°C^{-1}$. The convergence velocity v between the descending slab and the overriding lithosphere is one of the input parameters of the model. It can be inferred from the low heat flow in the arc-trench region (see below), that heat transport for the area above the slab is caused by conduction only and that no subduction induced flow of mantle material above the slab takes place in the arc-trench region. Thus velocities for the area above the slab are assumed to be zero. Adiabatic compression ($(\partial T/\partial t)_{ad}$ in Equation 1) causes an increase in temperature of 20–40° C for an increase in depth of 100 km. A is the heat production, as a consequence of friction and the decay of radioactive elements, per unit volume.

Finite difference methods are used to solve Equation 1 numerically. Time dependent solutions of the temperatures at gridpoints are calculated, using Runge-Kutta formulas, by a procedure described in Verwer (1977). The boundary condition at the surface is T = 0° C. Temperatures for the downbending oceanic lithosphere below the trench (x = 0 km) are calculated for a boundary layer model from Crough (1975), described in Wortel (1980), with a temperature of 1325° C at the base of the oceanic lithosphere. Temperatures below the volcanic line, at depths less than 90 km, are those of a geotherm with a surface heat flow of 80 mW m^{-2}. Temperatures are about 820, 1240 and 1355° C at depths of 30, 60 and 90 km. Such a high heat flow is common for the volcanic zone and the back-arc region (see also Fig. 3). Also high temperatures below the volcanic zone can be inferred from the composition of arc basalt magmas (Tatsumi et al. 1983). Migration, if any, of a volcanic zone is very slow (Dickinson 1973).

Frictional heat production

Interaction between the two plates leads to a zone of thrust earthquakes. This zone extends to a depth of 60–70 km (Isacks & Molnar 1971). Large thrust earthquakes do not occur near the trench at depths less than about 15 km (Yoshii 1979). It is probable that significant heat production by friction will only take place in the zone of thrust earthquakes. In the thermal model, shear stress (and thus heat production by friction) increases linearly with depth for depths less than 25 km. At depths between 25 and 75 km the shear stress is taken to be constant; the magnitude of this shear stress is one of the input parameters of the model. Below a depth of 75 km the shear stress is assumed to be zero.

Friction causes a heat production (per unit volume) A_f:

$$A_f = \frac{V\tau}{z_f} \qquad (2)$$

where z_f is the thickness of the deformation zone (6 km in the model) and τ the shear stress. The effect of friction on temperatures is governed by the product of the convergence velocity and the shear stress, which has the dimension of heat flow. Most of the heat that is generated is used to heat the cold upper part of the descending slab.

Radiogenic heat production

A substantial part of the heat flow at the surface is caused by the decay of radioactive elements, concentrated in sediments and crustal material. Crust in the arc-trench region can be of various origin. Radiogenic heat production in crust of oceanic origin is low; a characteristic heat production of 0.5 μW m^{-3} leads to a contribution of 5–10 mW m^{-2} (for crustal thicknesses of 10–20 km). Crust formed by subduction related volcanism (arc crust) has a low typical heat production of 0.25–0.50 μW m^{-3} (Gill 1981: 45). For an arc crust with a thickness of 30 km, the resulting contribution to the surface heat flow is 8–15 mW m^{-2}. The upper part of continental crust will have a much higher radiogenic heat production (typically 2.5 μW m^{-3}; Pollack & Chapman, 1977); it is estimated that the probably thin continental crust in an arc-trench region will not give a contribution greater than 25 mW m^{-2}.

Sediments in the forearc basin are derived from arc crust near the volcanic zone (Dickinson 1974) and are thus expected to give a low contribution to the surface heat flow (<5 mW m^{-2} for a sediment thickness less than 10 km). Heat production in the

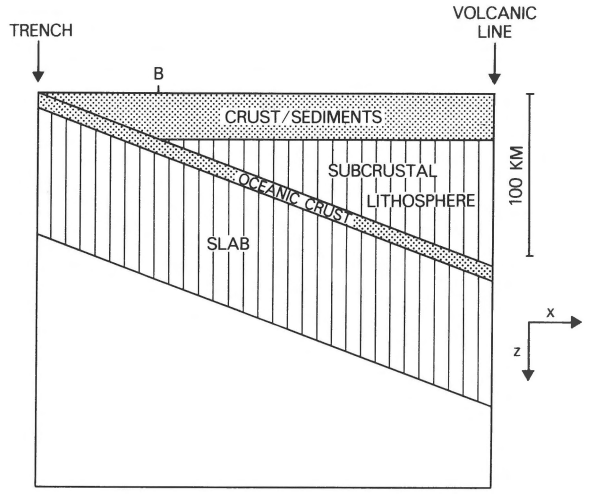

Fig. 2. Geometry of the model. The depth of the slab below the volcanic line is 105 km. The vertical scale is equal to the horizontal scale.

accretionary wedge, consisting of offscraped deep sea sediments may be much higher, resulting in a maximum contribution of 20 mW m^{-2} for an accretionary wedge with a sediment thickness of 15 km (Oxburgh & Turcotte 1971).

In an arc-trench region the following sequence generally exists (in the direction from the trench to the volcanic line; see also Fig. 1): accretionary wedge – oceanic crust and forearc sediments – arc crust and/or continental crust (Dickinson & Seely 1979). Although the radiogenic contribution to the heat flow will vary significantly in the arc-trench region, it is probably everywhere between 10 and 25 mW m^{-2} (except in the region near the trench, where the accretionary wedge is very thin).

In the model, heat production decreases exponentially with depth for the crustal part of the overriding lithosphere (with d equal to 12 km; Jaupart et al. 1981):

$$A_r(z) = A_O \exp(-z/d) \qquad (3)$$

For the region between B and the volcanic line (see Fig. 2), this results in a heat flow Q_r:

$$Q_r = \int_0^h A_O \exp(-z/d)dz \qquad (4)$$

where h is the thickness of the crust in this region (including sediments) which is taken to be 30 km. Q_r is one of the input parameters of the model and has been varied between 10 and 25 mW m^{-2}.

Heat flow in the arc-trench region

Heat flow measurements (from Anderson 1980; Nakamura & Wakita 1982 and Yoshii 1983) for the subduction zone near the Japan trench (N.E. Honshu) are given in Figure 3. Heat flow is low in the entire arc-trench region; most data points fall below a level of 40 mW m^{-2}. The volcanic line is associated with an increase in heat flow to 75–100 mW m^{-2} over a relatively short distance.

Heat flow in other subduction zones falls in a similar pattern; low heat flow (generally less than 40 mW m^{-2}) in the arc-trench region and high heat flow in the volcanic zone and the back-arc region.

Table 1. Heat flow in the central part of arc-trench regions.

Subduction zone	Heat flow[a] (in mW m^{-2})	Duration[b] (in Ma)
N.E. Honshu	34 ± 2	>100
S.W. Honshu	53 ± 3	± 15
Kuriles	33 ± 5	>100
Izu-Bonin	43 ± 9	± 40
South America	35 ± 5	>100
Central America	30 ± 5	>100
Cascades (Oregon)	36 ± 3	>100
Cascades (Brit. Columbia)	31 ± 6	>100

a: Average values for heat flow measurements at distances greater than $0.25 \times X_{AT}$ (where X_{AT} is the total distance between the trench and the volcanic line). Heat flow data from Anderson 1980 (N.E. Honshu, Izu-Bonin); Blackwell et al. 1977 (Central America); Blackwell et al. 1982 (Cascades, Oregon); Henry 1981 (South America); Hyndman 1976 (Cascades, British Columbia); Nakamura & Wakita 1982 (N.E. Honshu); (Uyeda & Watanabe 1982 (South America); Watanabe et al. 1977 (S.W. Honshu, Kuriles); Yoshii 1983 (N.E. Honshu). Also given are standard deviations for the average values.

b: Duration since the initiation of subduction, taken or inferred from Coney & Reynolds 1978 (Cascades); Hilde et al. 1977 (N.E. Honshu, Izu-Bonin, Kuriles); Karig et al. 1978 (Central America); Kobayashi 1983 (S.W. Honshu); Palacios 1984 (South America). These durations are in agreement with the ages of the oldest volcanic rocks for a number of subduction zones, given by Dickinson (1973).

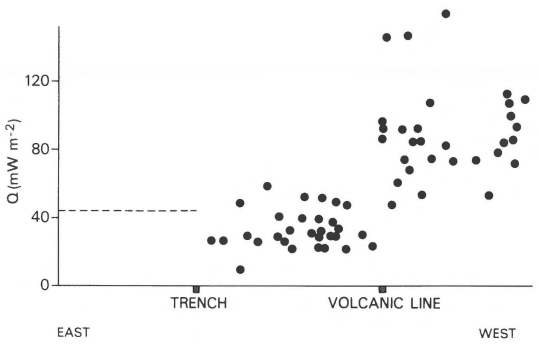

Fig. 3. Heat flow for the subduction zone near the Japan trench (N.E. Honshu). Heat flow data from Anderson (1980); Nakamura and Wakita (1982) and Yoshii (1983). The dashed line is the theoretical heat flow (for a boundary layer model from Crough (1975)) for oceanic lithosphere with an age of 120 Ma. This is the age of the descending Pacific plate at the Japan trench. Distance between the trench and the volcanic line is about 270 km.

Average values of the heat flow measurements in the central part of the arc-trench region for a number of subduction zones are listed in Table 1. Data at distances less than $0.25 \times X_{AT}$ from the trench or the volcanic line are excluded (where X_{AT} is the total distance between the trench and the volcanic line). Despite the large spread in the individual heat flow data, the differences in these average values are quite small. The large variations in the current convergence velocity (3 cm/a for the Cascades; 11 cm/a for South America) and the current age of the subducting oceanic lithosphere (10 Ma for the Cascades; 120 Ma for N.E. Honshu) are apparently of little influence.

Average values higher than 40 mW m^{-2} are only reached for the Izu-Bonin and S.W. Honshu subduction zones. Note that the error in the average value for the Izu-Bonin subduction zone is relatively large. The time passed since the initiation of subduction is relatively short for these two subduction zones (see Table 1). This may lead to a higher heat flow, since it will take time for the lithosphere above the slab to cool, after the initiation of subduction. All other subduction zones have been active for more than 100 Ma. Average values of heat flow in the central part of the arc-trench region for these subduction zones range from 30 to 36 mW m^{-2}. During model calculations this interval is used as a constraint for the heat flow of older subduction zones.

All older subduction zones have a sharp increase in heat flow in the direct vicinity of the volcanic line. For some of these subduction zones heat flow in the arc-trench region at distances less than about 60 km from the volcanic line is somewhat higher than in the central part of the arc-trench region (on the average about 8 mW m^{-2} for the Cascades). This could be caused, via horizontal conduction, by the high temperatures behind the volcanic line.

Model calculations

As a starting point for the model calculations a convergence velocity v is chosen of 8 cm/a; an age T_{sl} of the oceanic lithosphere at the trench of 70 Ma and a radiogenic heat flow Q_r of 17 mW m^{-2}. The values of T_{sl} and v are chosen in such a way, that they are close to the average values of these parameters for subduction zones. The value of Q_r lies in the middle of the interval 10–25 mW m^{-2}. In order to investigate the effect of friction, model calculations have been made for three values of τ; 0, 40 and 80 MPa. Note that these values represent the shear stress at depths between 25 and 75 km.

Figure 4 gives the heat flow for these three models (ATa0, ATa40 and ATa80), 100 Ma after the initiation of subduction. At this time a stable situation is almost completely reached (see Fig. 6); still longer model calculations give differences in temperature that are less than 5° C everywhere. The model with a shear stress of 40 MPa has a heat flow which falls within the interval (30–36 mW m^{-2}) inferred from heat flow data for the central part of the arc-trench region; the other two models have a significantly lower or higher heat flow. The thermal structure of the model with a shear stress of 40 MPa (model ATa40) is given in Figure 5.

The main part of the heat produced by friction is used to heat the cold upper part of the descending slab. For model ATa40 only 10–15% of the heat flow, caused by friction, goes upward and contributes to the surface heat flow. This is sufficient, however, for friction to be of vital importance for the temperatures in the lithosphere above the slab.

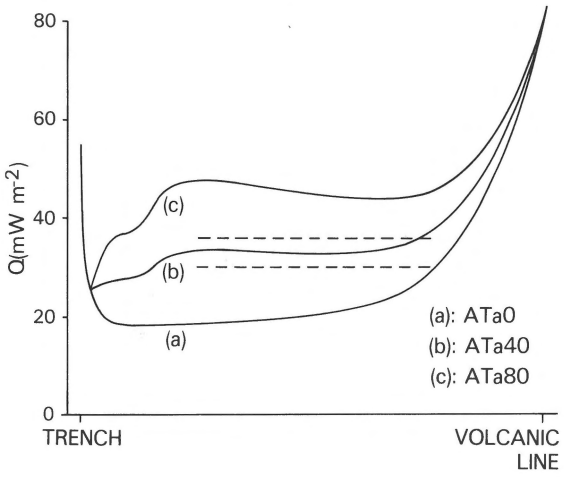

Fig. 4. Heat flow for the models ATa0, ATa40 and ATa80, 100 Ma after the initiation of subduction. The dashed lines give the interval inferred from heat flow data (30–36 mW m^{-2}). The heat flow of about 55 mW m^{-2} at the trench is the heat flow for oceanic lithosphere prior to subduction. Distance between the trench and the volcanic line is about 285 km.

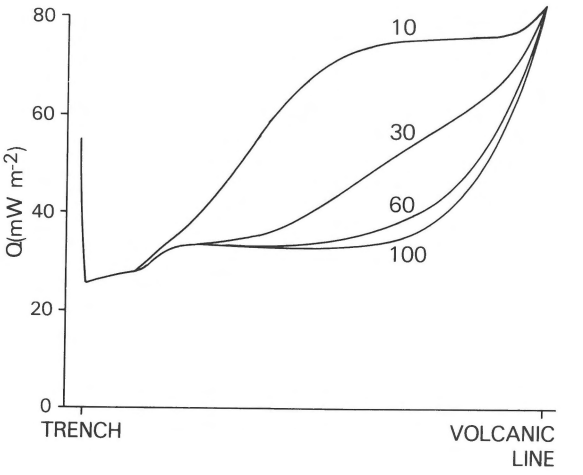

Fig. 6. Heat flow for model ATa40 at 10, 30, 60 and 100 Ma after the initiation of subduction.

Temperatures for the model without frictional heating are about a factor 2 lower here.

Heat flow profiles for model ATa40 at 10, 30, 60 and 100 Ma after the initiation of subduction are given in Figure 6. During the first 60 Ma the heat flow is significantly higher than that of the stable situation. Thus the gradual cooling of the lithosphere above the slab can explain higher heat flow values for the Izu-Bonin and S.W. Honshu subduction zones.

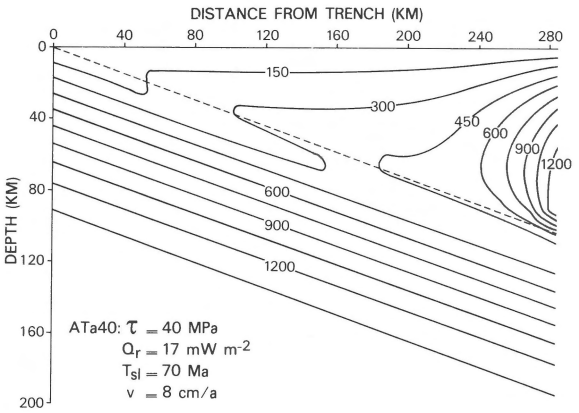

Fig. 5. Thermal structure of the region between the trench and the volcanic line for model ATa40; 100 Ma after the initiation of subduction.

Variation of model parameters

The thermal structures, 100 Ma after the initiation of subduction, for models with values for Q_r of 25 mW m^{-2} (model ATb20) and 10 mW m^{-2} (model ATc60) are given in Figure 7. Shear stresses are of such a magnitude that the steady state heat flow lies between 30 and 36 mW m^{-2} in the central part of the arc-trench region (20 MPa for model ATb20 and 60 MPa for model ATc60). Thus model ATb20 gives a low estimate of the temperatures in the arc-trench region and model ATc60 gives a high estimate. The differences in temperature for these models are primarily caused by differences in shear stress; the influence of Q_r is smaller and limited to the temperatures near the surface.

Numerical calculations have shown that variations of T_{sl} and v have only a small effect on temperatures above the slab. For model ATa40 an increase of T_{sl} from an average value of 70 Ma to a very high value of 150 Ma or a low value of 30 Ma has about the same effect on the temperatures above the slab as a decrease or increase in shear stress of about 4 MPa. An increase in convergence velocity causes an increased cooling by the cold upper part of the slab; but also a greater heat production by friction (Equation 2). The net effect turns out to be small; calculations with velocities of

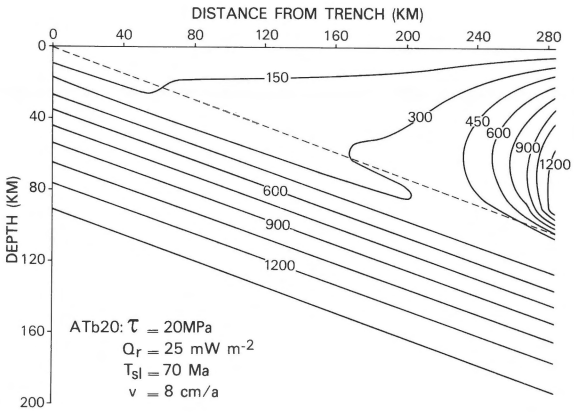

Fig. 7a. Thermal structure for model ATb20; 100 Ma after the initiation of subduction.

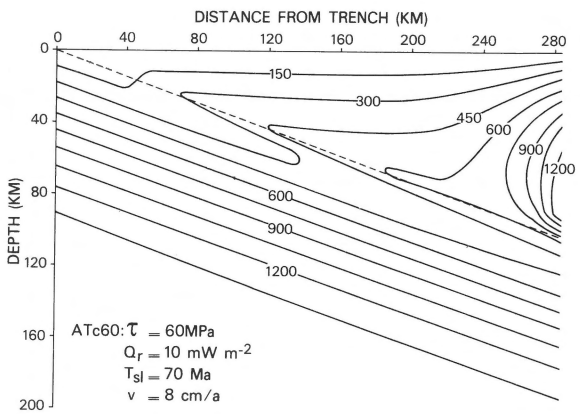

Fig. 7b. Thermal structure for model ATc60; 100 Ma after the initiation of subduction.

5 and 11 cm/a (other parameters the same as in model ATa40) give differences in heat flow that are less than 2 mW m^{-2} everywhere.

It can be concluded, that the temperatures above the slab and at the upper surface of the slab are primarily determined by frictional heating. If heat flow data are used as a constraint, the uncertainty in the estimate of the shear stress is determined by the uncertainty in Q_r.

High-pressure metamorphism

Subduction of oceanic lithosphere can lead to the formation of an accretionary wedge, which consists of sedimentary material. In a high-pressure metamorphic belt, such as the Franciscan complex of California, the deeper parts of a former accretionary wedge are exposed (Oxburgh & Turcotte 1971; Miyashiro 1973). A high-pressure metamorphic belt is characterised by the following metamorphic facies (Ernst 1975, 1977): zeolite – prehnite and pumpellyite – blueschist and/or greenschist. The increasing metamorphic grade is caused by the increasing depth, that is reached by the material. Especially the occurrence of blueschists points to low temperatures, lower for instance than those of a shield geotherm. These low temperatures (at relatively high pressures) can probably only occur in a subduction zone environment.

Ernst (1977) derives, from observed mineral assemblages and experimentally determined or calculated phase equilibria, prograde p-T trajectories. Since sedimentary accretionary wedge material in downward movement is expected to be close to the upper surface of the descending slab (Cloos 1982), these trajectories represent temperatures during subduction at or just above the upper surface of the slab. Figure 8 gives such temperatures for the Franciscan complex in California. Also temperatures at

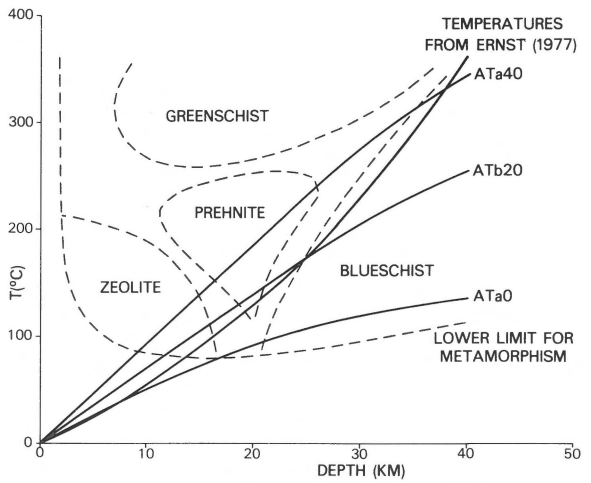

Fig. 8. Temperatures at the upper surface of the descending slab, as a function of depth, for models ATa40, ATb20 and ATa0. Also given are boundaries for metamorphic facies for temperatures below ±350 °C from Turner (1968) and prograde temperatures for high-pressure metamorphism in the Franciscan complex of California (from Ernst (1977); pressures are converted to depths, assuming a density of 2.7 kg m^{-3}).

the upper surface of the slab are given for the models ATa40 ($\tau = 40$ MPa), ATb20 ($\tau = 20$ MPa) and ATa0 ($\tau = 0$ MPa, hence no heat production by friction). Temperatures for the Franciscan complex are in reasonable agreement with those of the models ATa40 and ATb20. At depths greater than 20 km, the temperatures for the model without heat production by friction are much lower.

Wang & Shi (1984) have modelled temperatures for an accretionary wedge, assuming no frictional heating. For a velocity of 10 cm/a, their models show temperatures in the lower part of the accretionary wedge which are also much below those inferred for the Franciscan complex.

Discussion

An obvious limitation of thermal models of subduction zones is the constant dip of the slab. In this model of the arc-trench region a constant dip is chosen of 20°. In this way a better approximation of the geometry of the slab in an arc-trench region is obtained, than in models of a subduction zone as a whole, which generally use a constant dip of 45°. For depths below 30–40 km, however, the actual dip of the slab is usually even smaller than 20°. Also it is not clear, how shear stress increases with depth in the upper 30–40 km. In the model it is assumed that, for depths less than 25 km, shear stress increases linearly with depth. In reality the way shear stress increases with depth will be more complicated and depend for instance on pore-fluid pressures and whether the slab is in contact with the accretionary wedge or with the overriding lithosphere. Thus no accurate estimate of shear stresses can be made on the bases of temperatures inferred for high-pressure metamorphic belts alone. It does seem clear, however, that temperatures of $\pm 400°$ C at a depth of ± 40 km, inferred for high-pressure metamorphic conditions in a subduction zone environment (e.g. Ernst (1977) and Cloos (1985) for the Franciscan complex; Ernst (1981) and Gillet et al. (1985) for early Alpine metamorphism), can only be reached if significant heat production by friction, with shear stresses similar to those in the models ATa40 and ATb20, takes place.

Endothermic dehydration reactions for water-containing minerals in the crust of the descending slab will influence the thermal structure (Anderson et al. 1978). Major dehydration reactions in the crust of the slab, however, do not take place at depths less than about 75 km (Delaney & Helgeson 1978). The influence of these reactions is thus limited to temperatures in the upper part of the slab below this depth. The heat needed for the reactions will be readily supplied by the nearby asthenospheric wedge.

The magnitude of shear stresses depends on the rheological properties of the material near the upper surface of the slab and a number of parameters such as pressure, temperature and pore-fluid pressure. Large interplate thrust earthquakes at the upper surface of the descending slab occur between depths of 20 and 40 km (Ruff & Kanamori 1983) and this points to brittle deformation at these depths. For brittle deformation the strength of the material will be much reduced if high pore-fluid pressures exist (Kirby 1983). High pore-fluid pressures are likely for the accretionary wedge (Davis et al. 1983; von Huene 1984) and the crust of the slab, which consists for a substantial part of water-containing minerals. This may explain why shear stresses, inferred from heat flow data, are relatively low; about a factor 10 lower than those inferred from experiments under dry conditions (10^2–10^3 MPa; Byerlee 1978). The absence of interplate thrust earthquakes at depths below 60–70 km probably indicates that below this depth ductile deformation in the crust of the slab leads to low shear stresses.

Bird (1978) gives an estimate of 20 MPa for the average shear stress for depths less than 100 km. This estimate is based on a force balance for two subduction zones where back-arc spreading occurs (Tonga and Mariana subduction zones). Average shear stresses for depths less than 100 km for the models ATa40, ATb20 and ATc60 vary from 13 to 37 MPa, which is in reasonable agreement with Bird's estimate.

Volcanism

Generally subduction of oceanic lithosphere is associated with volcanism. Linear chains of volcanoes lie parallel to most of the ocean trenches. Volcanism is concentrated at the volcanic line; in the direction away from the trench the volume of erupted magmas decreases sharply (Sugimura 1968; Marsh 1979). Two possibilities are proposed for the first step of the process that leads to volcanism (e.g. Wyllie 1979; Gill 1981). Partial melting may occur in the crust of the slab, which requires temperatures above the wet solidus for basalt. At a depth of about 100 km this solidus lies near 750° C (Lambert & Wyllie 1972). An alternative is, that dehydration reactions in the crust are followed by upward migration of water and melting of hot mantle material above the slab. In both cases, however, melting is caused by the high temperatures in the asthenospheric wedge above the slab. This is in agreement with the absence of volcanism in segments of the South American subduction zone, where the dip of the slab is very small (<5°) at a depth of about 100 km, and the asthenospheric wedge is absent (Barazangi & Isacks 1979).

Friction does not lead to melting in the crust of the slab, within the region of our thermal models. Temperatures at the top of the slab below the volcanic line vary between ± 600° C (model ATb20) and ± 730° C (model Atc60). Essential, however, is the depth to which the boundary condition below the volcanic line continues. For these models this depth lies about 15 km above the top of the slab. Melting does take place if this boundary condition continues up to about 5 km above the slab.

Heat flow for older subduction zones is low (<40 mW m^{-2}) in the entire arc-trench region. Thus temperatures between the surface and the slab are much below mantle temperatures in the arc-trench region. This rules out convective processes in this area and heat transport is thus determined by conduction only. Temperatures in the back-arc region are high, as can be inferred from heat flow data (e.g. Fig. 3); generally the thickness of the lithosphere in this region is 50–75 km. Temperatures between the slab and the overriding lithosphere below the volcanic zone are also high; temperatures near 1400° C directly below the lithosphere near the volcanic zone are inferred by Tatsumi et al. (1983) from the composition of arc basalt magmas. It thus seems likely that the volcanic line marks the boundary of the asthenospheric wedge.

Conclusions

From published heat flow measurements it can be inferred that heat flow in the arc-trench region of older subduction zones (subduction started more than about 60 Ma ago) is low: less than 40 mW m^{-2}. Average heat flow values in the central part of the arc-trench region for a number of these subduction zones vary from 30 to 36 mW m^{-2}.

From our numerical calculations we conclude that a shear stress of 20–60 MPa along the plate contact, at depths between 25 and 75 km, is required to satisfy the heat flow data. Heat production by friction has a large influence on the temperatures in the arc-trench region. The influence of the age of the subducting oceanic lithosphere and the convergence velocity is relatively small. Gradual cooling of the region above the slab can explain higher heat flow in the arc-trench region for subduction zones, where subduction started less than about 60 Ma ago.

Temperatures inferred from mineral assemblages in high-pressure metamorphic belts can only be reached if significant heat is produced by friction. Calculated temperatures at the upper surface of the slab for the models satisfying the heat flow data are in reasonable agreement with temperatures inferred from mineral assemblages.

The volcanic line probably marks the boundary of the asthenospheric wedge.

References

Anderson, R.N. 1980 1980 Update of heat flow in the East and Southeast Asian seas. In: D.E. Hayes (ed): The tectonic and geologic evolution of Southeast Asian seas and islands, Geophys. Monogr. 23, Am. Geophys. Un., Washington D.C.: 319–326

Anderson, R.N., S.E. DeLong & W.M. Schwarz 1978 Thermal model for subduction with dehydration in the downgoing slab – J. Geol. 86: 731–739

Anderson, R.N., S.E. DeLong & W.M. Schwarz 1980 Dehydration, asthenospheric convection and seismicity in subduction zones – J. Geol. 88: 445–451

Anderson, R.N., S. Uyeda & A. Miyashiro 1976 Geophysical and geochemical constraints at converging plate boundaries, Part I: Dehydration in the downgoing slab – R. Astr. Soc. Geophys. J. 44: 333–357

Andrews, D.J. & N.H. Sleep 1974 Numerical modelling of tectonic flow behind island arcs – R. Astr. Soc. Geophys. J. 38: 237–251

Barazangi, M. & B.L. Isacks 1979 Subduction of the Nazca plate beneath Peru: evidence from spatial distribution of earthquakes – R. Astr. Soc. Geophys. J. 57: 537–555

Bird, P. 1978 Stress and temperature in subduction shear zones – R. Astr. Soc. Geophys. J. 55: 411–434

Blackwell, D.D., R.G. Bowen, D.A. Hull, J. Riccio & J.L. Steele 1982 Heat flow, arc volcanism, and subduction in Northern Oregon – J. Geophys. Res. 87: 8735–8754

Blackwell, D.D., J. Ziagos & F. Mooser 1977 Heat flow and the thermal effects of subduction in Southern Mexico – EOS Trans. Am. Geophys. Un. 58: 1233

Byerlee, J.D. 1978 Friction of rocks – Pure Appl. Geophys. 116: 615–626

Cloos, M. 1982 Flow melanges: numerical modelling and geologic constraints on their origin in the Franciscan subduction complex, California – Geol. Soc. Am. Bull. 93: 330–345

Cloos, M. 1985 Thermal evolution of convergent plate margins: thermal modelling and reevaluation of isotopic Ar-ages for blueschists in the Franciscan complex of California – Tectonics 4: 421–434

Coney, P.J. & S.J. Reynolds 1978 Overview of Mesozoic-Cenozoic Cordilleran plate tectonics. In: Smith, R.B. & G.P. Eaton (eds): Cenozoic tectonics and regional geophysics of the western Cordillera – Geol. Soc. Am. Memoir 152: 51–92

Crough, S.T. 1975 Thermal model of oceanic lithosphere – Nature 256: 388–390

Davis, D., J. Suppe & F.A. Dahlen 1983 Mechanics of fold-and-thrust belts and accretionary wedges – J. Geophys. Res. 88: 1153–1172

Delany, J.M. & H.C. Helgeson 1978 Calculation of the thermodynamic consequences of dehydration in subducting oceanic crust to 100 kbar and 800° C – Am. J. Sci. 278: 638–686

Dickinson, W.R. 1973 Widths of modern arc-trench gaps proportional to past duration of igneous activity in associated magmatic arcs – J. Geophys. Res. 78: 3376–3389

Dickinson, W.R. 1974 Sedimentation within and beside ancient and modern magmatic arcs. In: Modern and ancient geosynclinal sedimentation – SEPM Spec. Pub. 19: 230–239

Dickinson, W.R. & D.R. Seely 1979 Structure and stratigraphy of forearc regions – Am. Assoc. Petrol. Geol. Bull. 63: 2–31

Ernst, W.G. 1975 Systematics of large-scale tectonics and age progressions in Alpine and circumpacific blueschist belts – Tectonophysics 26: 229–246

Ernst, W.G. 1977 Mineral parageneses and plate tectonic settings of relatively high-pressure blueschist belts – Fortschr. Mineral. 54: 192–222

Ernst, W.G. 1981 Petrogenesis of eclogites and peridotites from the Western and Ligurian Alps – Am. Mineral. 66: 443–472

Furlong, K.P., D.S. Chapman & P.W. Alfeld 1982 Thermal modelling of the geometry of subduction with implications for the tectonics of the overriding plate – J. Geophys. Res. 87: 1786–1802

Gill, J. 1981 Orogenic andesites and plate tectonics. Springer, Berlin, 390 pp

Gillet, P., P. Davy, M. Ballèvre & P. Choukroune 1985 Thermomechanical evolution of a collision zone: the example of the Western Alps – Terra Cognita 5: 399–404

Henry, S.G. 1981 Terrestrial heat flow overlying the Andean subduction zone – Ph. D. Thesis, Univ. of Michigan, Ann Arbor, 194 pp

Hilde, T.W.C., S. Uyeda & L. Kroenke 1977 Evolution of the western Pacific and its margin – Tectonophysics 38: 145–165

Honda, S. 1985 Thermal structure beneath Tohoku, Northeast Japan. A case study for understanding the detailed thermal structure of the subduction zone – Tectonophysics 112: 69–102

Honda, S. & S. Uyeda 1983 Thermal process in subduction zones, a review and preliminary approach on the origin of arc volcanism. In: Shimozura, D. & I. Yokoyama (eds): Arc volcanism: physics and tectonics, Tokyo: 117–140

Hsui, A.T. & M.N. Toksöz 1979 The evolution of thermal structures beneath a subduction zone – Tectonophysics 60: 43–60

Hyndman, R.D. 1976 Heat flow measurements in the inlets of Southwestern British Columbia – J. Geophys. Res. 81: 337–349

Isacks, B.L. & M. Barazangi 1977 Geometry of Benioff zones: lateral segmentation and downwards bending of subducted lithosphere. In: Talwani, M. & W.C. Pitman, III (eds): Island arcs, deep sea trenches and back-arc basins, Maurice Ewing series 1, Am. Geophys. Un., Washington D.C.: 99–114

Isacks, B.L. & P. Molnar 1971 Distribution of stresses in the descending lithosphere from a global survey of focal mechanism solutions of mantle earthquakes – Rev. Geophys. Space Phys. 9: 103–174

Jaupart, C., J.G. Sclater & G. Simmons 1981 Heat flow studies: constraints on the distribution of uranium, thorium and potassium in the continental crust – Earth Planet. Sci. Lett. 52: 328–344

Karig, D.E., R.K. Caldwell, G.F. Moore & D.G. Moore 1978 Late Cenozoic subduction and continental-margin truncation along the northern Middle America trench – Geol. Soc. Am. Bull. 89: 265–276

Kirby, S.H. 1983 Rheology of the lithosphere – Rev. Geophys. Space Phys. 21: 1458–1487

Kobayashi, K. 1983 Fore-arc volcanism and cycles of subduction. In: Shimozura, D. & I. Yokoyama (eds): Arc volcanism: physics and tectonics, Tokyo: 153–163

Lambert, I.B. & P.J. Wyllie 1972 Melting of gabbro (quartz eclogite) with excess water to 35 kilobars, with geological

applications – J. Geol. 80: 693–720
Marsh, B.D. 1979 Island-arc volcanism – Am. Scientist 67: 161–172
Minear, J.W. & M.N. Toksöz 1970 Thermal regime of a downgoing slab and new global tectonics – J. Geophys. Res. 75: 1397–1419
Miyashiro, A. 1973 Metamorphism and metamorphic belts. Allen & Unwin, London, 492 pp
Nakamura, Y. & H. Wakita 1982 Terrestrial heat flow around the aseismic front of the Japanese island arc – Tectonophysics 81: T25–T36
Oxburgh, E.R. & D.L. Turcotte 1971 Origin of paired metamorphic belts and crustal dilation in island arc regions – J. Geophys. Res. 76: 1315–1327
Palacios, C.M. 1984 Considerations about the plate tectonic model, volcanism and continental crust in the southern part of the central Andes – Tectonophysics 106: 205–214
Pollack, H.N. & D.S. Chapman 1977 On the regional variation of heat flow, geotherms, and lithospheric thickness – Tectonophysics 38: 279–296
Ruff, L. & H. Kanamori 1983 Seismic coupling and uncoupling at subduction zones – Tectonophysics 99: 99–117
Schatz, J.F. & G. Simmons 1972 Thermal conductivity of earth materials at high temperatures – J. Geophys. Res. 77: 6966–6983
Sugimura, A. 1968 Spatial relations of basaltic magmas in island arcs. In: Hess, H.H. & A. Poldevaart (eds), Basalts, vol II, Wiley Interscience Publ., New York: 537–571
Sydora, L.J., F.W. Jones & R. Lambert 1980 Model calculations of the thermal fields of subducting slabs and partial melting – Tectonophysics 62: 233–250
Tatsumi, Y., Sakuyama, M., Fukuyama, H. & I. Kushiro 1983 Generation of arc basalt magmas and thermal structure of the mantle wedge in subduction zones – J. Geophys. Res. 88: 5815–5825
Turcotte, D.L. & G. Schubert 1973 Frictional heating of the descending lithosphere – J. Geophys. Res. 78: 5876–5886
Turner, F.J. 1968 Metamorphic petrology. New York, McGraw-Hill, 524 pp
Uyeda, S. & T. Watanabe 1982 Terrestrial heat flow in western South America – Tectonophysics 83: 63–70
Verwer, J.G. 1977 A class of stabilized three-step Runge-Kutta methods for the numerical integration of parabolic equations – J. Comp. Appl. Math. 3: 155–166
von Huene, R. 1984 Tectonic processes along the front of modern convergent margins – Ann. Rev. Earth Planet. Sci. 12: 359–381
Wang, C.Y. & Y.L. Shi 1984 On the thermal structure of subduction complexes; a preliminary study – J. Geophys. Res. 89: 7709–7718
Watanabe, T., M.G. Langseth & R.N. Anderson 1977 Heat flow in back-arc basins of the western Pacific. In: Talwani, M. & W.C. Pitman, III (eds): Island arcs, deep sea trenches and back-arc basins, Maurice Ewing series 1, Am. Geophys. Un., Washington D.C.: 137–160
Windley, B.F. 1984 The evolving continents. Wiley, Chichester, 399 pp
Wortel, M.J.R. 1980 Age-dependent subduction of oceanic lithosphere – Ph. D. Thesis, Univ. of Utrecht, Utrecht, 147 pp
Wyllie, P.J. 1979 Magmas and volatile components – Am. Mineral. 64: 469–500
Yoshii, T. 1979 A detailed cross section of the deep seismic zone beneath Northeast Honshu, Japan – Tectonophysics 55: 349–360
Yoshii, T. 1983 Cross sections of some geophysical data around the Japanese islands. In: Hilde, T.W.C. & S. Uyeda (eds): Geodynamics of the western Pacific-Indonesian region, Am. Geophys. Un., Washington D.C.: 343–354
Yuen, D.A., L. Fleitout, G. Schubert & C. Froidevaux 1978 Shear deformation zones along major transform faults and subducting slabs – R. Astr. Soc. Geophys. J. 54: 93–119